International Journal of Thermophysics, Vol. 10, No. 5, 1989

A Study of the Thermal Conductivity of Alumina/Glass Dispersed Composites[1]

M. L. Allitt,[2] A. J. Whittaker,[2] D. G. Onn,[2] and K. G. Ewsuk[3]

The thermal diffusivity of five groups of alumina/glass composite systems has been measured at room temperature using a laser flash system. These data have been used, in conjunction with specific heat and density measurements, to calculate the effective thermal conductivity of these composites. In each of the five groups a systematic variation in glass concentration was made, and each group represents systematic variations in glass and alumina particle sizes. The thermal conductivities calculated are compared with those predicted by four models. It is apparent from these comparisons that the geometry and orientation of porosity within the sample measured are a key factor in determining which of these models (if any) is appropriate for describing the thermal conductivity of these composites.

KEY WORDS: alumina; composites; glass; porosity; thermal conductivity; thermal diffusivity.

1. INTRODUCTION

As integrated circuits become faster and more densely packed, the need for new substrate materials grows. Due to the high frequencies at which modern microchips work, these substrates should have a low dielectric constant while also possessing an ability to dissipate efficiently the increased heat generated by such dense circuits. Of increasing interest are composites, comprising two different materials, each possessing one of the desired properties. The dielectric constant and thermal conductivity of such a composite depend upon the relative proportions of its constituent phases

[1] Paper presented at the Tenth Symposium on Thermophysical Properties, June 20–23, 1988, Gaithersburg, Maryland, U.S.A.

[2] Department of Physics and Astronomy, University of Delaware, Newark, Delaware 19716, U.S.A.

[3] E.I. du pont de Nemours & Company, Wilmington, Delaware 19898, U.S.A.

0195-928X/89/0900-1053$06.00/0

and so the material can be manufactured with properties from within a broad range.

The composites studied in this work all combine the relatively high thermal conductivity of alumina with the low dielectric constant of alkaline earth alumino-borate glass (AEAB). An advantage of this system is that high processing temperatures are not required—all samples were vacuum hot pressed at temperatures in the range 675–900°C in a 1.27-cm graphite die at 50 MPa. Over the five different series of composites studied, there are systematic variations in the particle sizes of both the glass and the alumina (see Table I) and within each series the volume ratio of glass to alumina was varied systematically.

2. EXPERIMENTAL RESULTS

2.1. Experimental Method

The thermal diffusivity, α, of each sample was measured by the laser flash method [5]. The density, ρ, of each sample was measured using Archimedes' principle [6]. Specific heat, C_p, was obtained using an electronic pulse technique [7] to measure directly the specific heat of a sample of fully dense alumina and of a sample of fully dense AEAB glass. The specific heat of intermediate compositions can then be obtained using the rule of mixtures.

With these data the thermal conductivity, K, of each sample can be calculated from the following relationship:

$$K = \alpha \rho C_p \tag{1}$$

The maximum total error in this calculated thermal conductivity is estimated to be $\pm 15\%$.

Table I. Median Particle Sizes of Composite Components: Series E is Series C Re-Pressed to a Greater Density

	Particle size (μm)	
Series	Alumina	Glass
A	1.5	2.9
B	3.2	1.7
C	3.2	2.6
D	0.4	2.6
E	3.2	2.6

2.2. Discussion of Experimental Results

The thermal conductivity values obtained as described above are plotted in Fig. 1 as a function of nominal alumina volume fraction. Note that this is not the true volume fraction of alumina present in the material, but a volume fraction computed as the ratio of the volume of alumina present to the total volume occupied by the alumina plus glass, i.e., the volume occupied by porosity is neglected.

The figure shows that all five series follow basically the same trend—the thermal conductivity rises with increased alumina content to some threshold value, which occurs in most cases at a nominal alumina volume fraction of 65–70%, after which a decrease is observed. Density measurements show that there is a rapid increase in the volume fraction of porosity present in the sample at this nominal alumina volume fraction. The figure also shows that there is little variation in the magnitude of the thermal conductivity between different series, for a given nominal alumina volume fraction. This indicates that neither the alumina particle size nor the glass particle size has a major effect on the final thermal conductivity of the composite.

3. COMPARISON WITH THEORY

3.1. Review of Analyses

3.1.1. The Maxwell Model

In steady state, the heat flow equation reduces to Laplace's equation:

$$\nabla^2 T = 0 \tag{2}$$

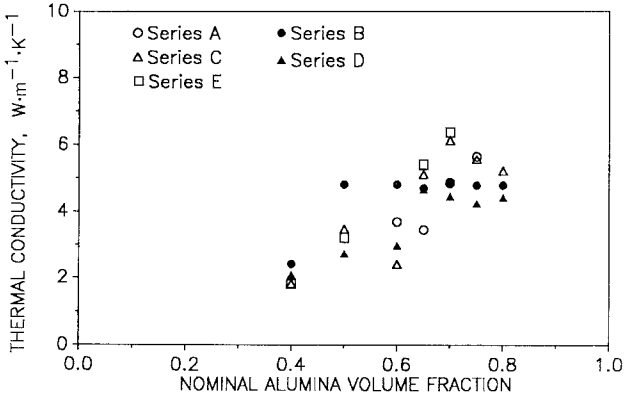

Fig. 1. Calculated thermal conductivity of alumina/glass composites.

where T is the temperature at any point in the material. Taking a picture of a composite of one type of spherical particle dispersed in a continuous phase of differing thermal conductivity, with the concentration of the dispersed phase low enough that the particles remain far enough apart so as not to interact with each other, potential theory can then be applied to Eq. (3) to yield the Maxwell [1] model:

$$K_e = K_c \left\{ \frac{K_d + 2K_c + 2V_d(K_d - K_c)}{K_d + 2K_c - V_d(K_d - K_c)} \right\} \tag{3}$$

where K_e is the effective composite thermal conductivity, K_d and V_d are the thermal conductivity and volume fraction of the discontinuous phase, respectively, and K_c is the thermal conductivity of the continuous phase. It has been shown by Ewsuk et al. [8] on the basis of this model that the thermal conductivity of alumina glass dispersed composites containing minimal porosity is dominated by the thermal conductivity of the continuous phase. Note that this model applies in this form only to two-phase systems.

3.1.2. The Kerner Model

Kerner [2] viewed the suspended, spherical particles of the discontinuous phase to be surrounded by a shell of the continuous phase. Sufficiently far from this shell the composite is on average a homogeneous medium with the same conductivity as the effective composite conductivity. Continuity demands that in between there is a region of variable and unknown conductivity. Kerner showed that for spherical inclusions the properties of this intermediate zone are unimportant and so derived a relationship for the effective composite conductivity valid for all volume fractions of dispersed phase less than 1:

$$K_e = \frac{\sum_{i=1}^{n} K_i V_i \dfrac{3K_1}{K_i + 2K_1}}{\sum_{i=1}^{n} V_i \dfrac{3K_1}{K_i + 2K_1}} \tag{4}$$

Here the label 1 refers to the continuous phase. Note that this model applies to any number, n, of dispersed, spherical phases within the continuous phase. For the case of one dispersed phase it reduces to the Maxwell model above.

3.1.3. The Clayton Model

Bruggeman [9] derived a model for the thermal conductivity of a spherical phase dispersed in a continuous matrix on the basis of an effective

medium theory similar to that later used by Kerner. A composite of thermal conductivity K_e is constructed from spherical inclusions dispersed in a continuous phase to yield an average effective medium. The small change in thermal conductivity of the composite arising from the further addition of an infinitesimal amount of the discontinuous phase is then calculated and an equation relating K_e to the concentrations and conductivities of the two phases present obtained by integration. Clayton [3] generalized this approach to allow for the possibility of the dispersed phase being of ellipsoidal geometry to give the following relationship:

$$1 - V_d = \frac{K_d - K_e}{K_d - K_c}\left(\frac{K_c}{K_e}\right)^{1/(x+1)} \tag{5}$$

where x is a factor designed to account for the shape of the inclusions. For spheres, $x = 2$.

The effective medium approximation used here neglects interparticle interactions in the same way as the Maxwell model, and so this approach is limited to dilute volume fractions. Again, note that this model is applicable only to two-phase systems.

3.1.4. The Hsu Model

Hsu and Berzins [4] have presented another effective medium approach. Starting with a homogeneous material of the required thermal conductivity, a composite of the desired composition is built up by replacing part of the original effective medium with a small amount of one of the phases (designated by the subscript 1), thus creating a change in the conductivity of the whole. A small part of the second phase (subscript 2) is then added in such a way as to return the composite conductivity to its original value. This process is continued until a composite of the desired composition has been created. This approach leads to the following equation:

$$\{1 - F(e)\}K_e^2 + \{K_1[F(e) - V_1] + K_2[F(e) - V_2]\}K_e - K_1K_2F(e) = 0 \tag{6}$$

where $F(e)$ is a function of the eccentricity of the dispersed phase and is designed to take into account the shape and orientation of this phase. For spheres, $F(e) = 1/3$. $F(e)$ is assumed to be the same for both phases, i.e., both phases are treated the same and we no longer have a picture involving a continuous matrix. One would therefore expect this model to be applicable in situations where matrix and filler both tend to cluster and form agglomerates within the composite. Again, this model is designed to be applied to two-phase composites.

3.2. Extension of Two-Phase Models to Three-Phase Systems

Three of the above four models are designed to apply only to two-phase systems. The alumina/glass materials measured in this work are three-phase systems, consisting of glass, alumina, and porosity phases. It is therefore apparent that some manipulation of these models is required in order to apply them to these materials.

Clayton presented a procedure for doing this with his analysis which was subsequently applied with success by Mottram and Taylor [10] and Whittaker [11] in studies of directionally reinforced fibrous composites. A similar method should be applicable to other analyses. The first step is to calculate the thermal conductivity of a nonporous composite, using as input parameters to the models the thermal conductivity of alumina, K_d, the thermal conductivity of AEAB glass, K_c, and putting the volume fractions of the dispersed and continuous phases V_d and V_c equal to the known nominal alumina and glass volume fractions V_f' and V_m', calculated from the known masses of these materials used and their measured densities. This yields a thermal conductivity K_e. The value used for K_c was measured experimentally to be $1.1\ W \cdot m^{-1} \cdot K^{-1}$. The value of K_d used, $30\ W \cdot M^{-1} \cdot K^{-1}$ represents an average of several literature results as reviewed by Ewsuk et al. [8] and is in broad agreement with measurements made on various other polycrystalline aluminas at the University of Delaware.

The value of K_e so obtained can then be regarded as the thermal conductivity of the continuous phase in another composite, containing porosity as the dispersed phase. Thus the same model can then be used again, with this time the input parameters being $K_d = 0$, $K_c = K_e$, and V_d equal to the porosity volume fraction V_p, with $V_c = 1 - V_p$. This procedure then yields a final effective thermal conductivity for the porous composite K_e', which can then be compared with the experimentally measured data. Applying this procedure to the Maxwell, Clayton, and Hsu models then gives the following relationships for the final, three-phase, composite thermal conductivity.

Maxwell:

$$K_e' = \frac{(1 - V_p)}{(1 + V_p/2)} K_e \tag{7}$$

Clayton:

$$K_e' = (1 - V_p)^{(x+1)/x} K_e \tag{8}$$

Hsu:

$$K_e' = \frac{1 - V_p - F(e)}{1 - F(e)} K_e \tag{9}$$

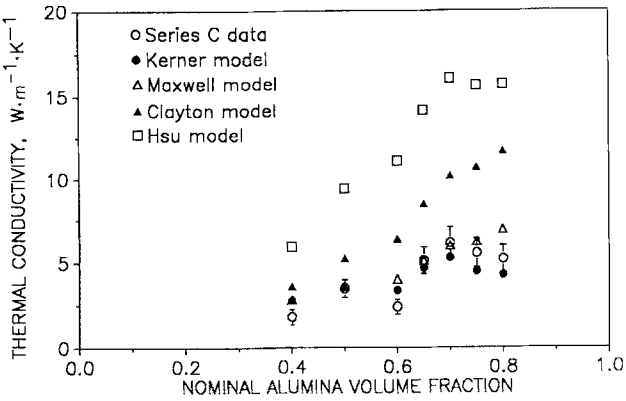

Fig. 2. Comparison of predictions of Maxwell, Kerner, Clayton, and Hsu models with the results for series C.

In all cases it is assumed that the porosity is present in the form of spherical voids in the matrix.

3.3. Comparison of Models with Experimental Data

Figure 2 shows a comparison of the predictions of the four models with the values obtained from measured data for the series C. The figure shows that the Hsu and Clayton models based on the assumptions outlined above do not fit the data well. However, the Maxwell and Kerner models give predictions much closer to the measured values. Figure 3 shows a

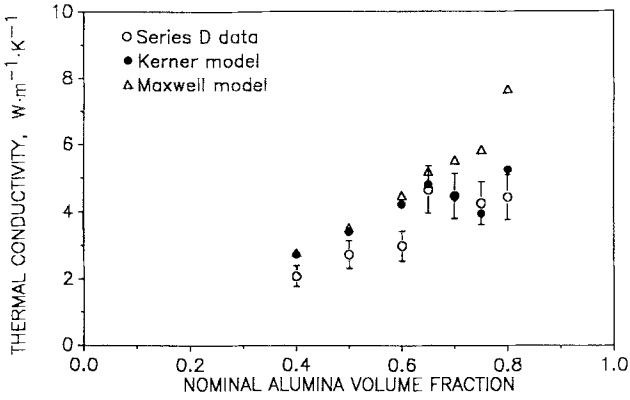

Fig. 3. Comparison of predictions of Maxwell and Kernel models with the results for series D.

comparison between the Kerner and Maxwell models and the experimental results for the series D. In general the Kerner model gives slightly better agreement with the data than does the Maxwell model and appears to follow the trends in the data closely; however, the predicted magnitudes are frequently at variance with those measured.

Table II. Calculated Values of the Porosity Shape Factors in the Hsu and Clayton Models that Will Bring the Predictions of These Models for Spherical Alumina in a Glass Matrix into Agreement with Experiment

		Model used for alumina in glass			
		Clayton		Hsu	
Sample	Nominal alumina volume fraction	x	F(e)	x	F(e)
A1	0.6	0.08	0.9	0.04	0.93
A2	0.65	0.06	0.92	0.04	0.94
A3	0.7	0.07	0.91	0.04	0.93
A4	0.75	0.14	0.82	0.09	0.86
B1	0.8	0.19	0.76	0.14	0.78
B2	0.75	0.23	0.73	0.15	0.77
B3	0.7	0.35	0.66	0.20	0.74
B4	0.65	0.32	0.69	0.16	0.78
B5	0.6	0.39	0.67	0.14	0.81
B6	0.5	0.31	0.76	0.03	0.96
B7	0.4	0.39	0.68	0.15	0.82
C1	0.8	0.22	0.73	0.16	0.76
C2	0.75	0.19	0.77	0.13	0.82
C3	0.7	0.10	0.89	0.05	0.92
C4	0.65	0.10	0.89	0.05	0.92
C5	0.6	0.11	0.84	0.07	0.87
C6	0.5	0.00	1.00	0.00	1.00
C7	0.4	0.01	0.98	0.01	0.99
D1	0.8	0.11	0.83	0.09	0.85
D2	0.75	0.20	0.75	0.14	0.78
D3	0.7	0.13	0.83	0.08	0.87
D4	0.65	0.06	0.92	0.04	0.94
D5	0.6	0.05	0.93	0.03	0.95
D6	0.5	0.03	0.96	0.02	0.97
D7	0.4	0.02	0.98	0.01	0.98
E1	0.7	0.08	0.9	0.04	0.94
E2	0.65	0.08	0.9	0.04	0.94
E3	0.5	0.04	0.95	0.02	0.97
E4	0.4	0.01	0.98	0.01	0.99

3.4. Porosity Shape Factors

Since none of the above models consistently fit the data well, the picture of spherical alumina particles and spherical pores dispersed in a continuous glass matrix is possibly too simplistic. The Hsu and Clayton models both contain parameters that are adjustable according to the shape and geometry of the dispersed phase. It is an interesting exercise to use these models for the porosity and to calculate the values that the shape factors need to have, sample by sample, in order to bring the predictions of any particular model into agreement with the experimental data. Table II shows calculated values of $F(e)$ and x for all samples that bring the predictions of the Clayton and Hsu models into agreement with the data. These shape factors show a remarkable consistency, in that there is not a great spread in the calculated values through a given series, and also for low nominal alumina volume fractions the shape factor is much the same for all series, particularly for $F(e)$ when using the Hsu model twice. This is perhaps not unreasonable since all the samples were manufactured by nominally the same technique.

The calculated values of $F(e)$ lie in the range 0.65 to 1, implying a porosity eccentricity of between 0.95 and 1, i.e., by this model the porosity is present as thin platelets oriented perpendicular to the direction of heat flow. Looking at the values calculated for the Clayton model shape parameter we see that its value varies in the range 0 to 0.4. This would imply that the c axis of the ellipsoidal pore is several times smaller than its other two axes, i.e., we again have the implication that porosity is present as thin platelets oriented perpendicular to the direction of heat flow. This result is not unreasonable, since the nature of the hot pressing technique is such that it is not impossible that some directionality is imparted to the system. Isotropic, spherical porosity is not necessarily to be expected. However, due to insufficient data on the microstructure of these materials, no conclusion can yet be drawn as to the accuracy of this analysis.

4. CONCLUSIONS

Evidently the evaluation of the abilities of the four models described above to describe the behavior of these systems is complicated by the presence of porosity within the samples measured. The results described above show that accurate characterization of the system microstructure is necessary in order to form conclusions as to the accuracy of these models. It is anticipated that such information will be obtained for these materials through SEM and also through dielectric constant measurements.

ACKNOWLEDGMENTS

This research was supported by The State of Delaware Research Partnership with E.I. du pont de Nemours & Company, Wilmington, Del. 19898. The authors express their appreciation to E. H. Kerner for many valuable discussions.

REFERENCES

1. H. S. Carslaw and J. C. Jaeger, *Conduction of Heat in Solids* (Oxford University Press, New York, 1959), 2nd ed., pp. 421–428.
2. E. H. Kerner, *Proc. Phys. Soc. Lond. Ser. B* **69**:802 (1956).
3. W. A. Clayton, AIAA/ASME paper no. 71-38 (1971).
4. W. Y. Hsu and T. Berzins, *J. Polym. Sci. Polym. Phys. Ed.* **23**:933 (1985).
5. W. J. Parker, R. J. Jenkins, C. P. Butler, and G. L. Abbott, *J. Appl. Phys.* **32**:1679 (1961).
6. C. Cawthorne and W. D. J. Sinclair, *J. Phys. E* **5**:531 (1971).
7. R. E. Giedd and D. G. Onn, Proc. 20th Ther. Conduct. Conf. Blacksburg, Va., Oct. 1987. *Therm. Cond.* **20** (Plenum Press, New York, 1989).
8. K. G. Ewsuk, L. W. Harrison, F. J. Walczak, M. L. Allitt, A.. J. Whittaker, and D. G. Onn, Presented at 90th annual meeting of the American Ceramic Society, Cincinatti, April 1988. *Bull. Am. Ceram. Soc.* **67**:645 (1988).
9. D. A. G. Bruggeman, *Ann. Phys. (Leipzig)* **24**:636 (1935).
10. T. Mottram and R. Taylor, (to be published).
11. A. J. Whittaker, Ph.D. thesis (UMIST, 1986).